

Seismic site-response characterization of high-velocity sites using advanced geophysical techniques: application to the NAGRA-Net

V. Poggi,^{1,2} J. Burjanek,^{1,3} C. Michel¹ and D. Fäh¹

¹Swiss Seismological Service, Institute of Geophysics, ETH Zurich, Switzerland. E-mail: poggi.valerio@gmail.com

²Global Earthquake Model foundation (GEM), Pavia, Italy

³Institute of Geophysics, Czech Academy of Sciences, Czech Republic

Accepted 2017 May 5. Received 2017 May 3; in original form 2016 August 30

SUMMARY

The Swiss Seismological Service (SED) has recently finalised the installation of ten new seismological broadband stations in northern Switzerland. The project was led in cooperation with the National Cooperative for the Disposal of Radioactive Waste (Nagra) and Swissnuclear to monitor micro seismicity at potential locations of nuclear-waste repositories. To further improve the quality and usability of the seismic recordings, an extensive characterization of the sites surrounding the installation area was performed following a standardised investigation protocol. State-of-the-art geophysical techniques have been used, including advanced active and passive seismic methods. The results of all analyses converged to the definition of a set of best-representative 1-D velocity profiles for each site, which are the input for the computation of engineering soil proxies (traveltime averaged velocity and quarter-wavelength parameters) and numerical amplification models. Computed site response is then validated through comparison with empirical site amplification, which is currently available for any station connected to the Swiss seismic networks. With the goal of a high-sensitivity network, most of the NAGRA stations have been installed on stiff-soil sites of rather high seismic velocity. Seismic characterization of such sites has always been considered challenging, due to lack of relevant velocity contrast and the large wavelengths required to investigate the frequency range of engineering interest. We describe how ambient vibration techniques can successfully be applied in these particular conditions, providing practical recommendations for best practice in seismic site characterization of high-velocity sites.

Key words: Joint inversion; Earthquake ground motions; Seismic noise; Site effects.

1 INTRODUCTION

Recordings from high-sensitivity seismological networks cannot be used at their full potential without properly accounting for the complexity and diversity of the seismic response at the location of (and nearby) the installations. Neglecting the effect of local geology on the ground motion or oversimplifying the complexity of the phenomenon might lead to an over- or underestimation of the ground motion predicted at the surface and at depth (e.g. Cotton *et al.* 2006). This is usually the case for several ground motion prediction equations (GMPEs), which have been calibrated and model the local seismic response by using single site parameters (e.g. Vs30; see Douglas 2003; Douglas & Edwards 2016), often disregarding the frequency-dependent nature of the phenomenon. Such bias influences the uncertainty level of the prediction, with a consequent effect on the reliability of seismic hazard calculations.

Although the influence of local geology is particularly relevant for soft sediment sites, where resonance amplification and non-linear phenomena may play an important role (e.g. Borcherdt 1970; Field *et al.* 1997), site effects are also observed at so-called ‘high-velocity’

sites (e.g. Tucker *et al.* 1984; Cranswick 1988), such as in rock and stiff soil conditions. Their impact on seismic hazard analysis, especially for sensitive facilities, is critical. Moreover, GMPEs consider usually idealized engineering bedrock as the reference conditions. As a matter of fact, this simplified bedrock model, consisting of a homogeneous half-space of constant seismic velocity, can hardly be observed at real sites. Weathering, fracturing and the effect of overburden pressure with increasing depth always lead to variations in the elastic properties along the profile. In these conditions, although sharp velocity contrasts are unlikely expected, velocity gradients are common, which are usually responsible for high frequency amplification (e.g. Boore & Joyner 1997). Ignoring such effects leads to biases in GMPEs. In particular, national seismic hazard maps are defined on rock conditions, and the characterization of those stiff-sites hosting seismic stations is therefore a task of high relevance for reliable calibration of the ground motion model.

The Swiss Seismological Service (SED, Schweizerischer Erdbebendienst) has been developing new techniques for site characterization and seismic response analysis, with a particular focus on the analysis of ambient vibrations (e.g. Fäh *et al.* 2001; Poggi &

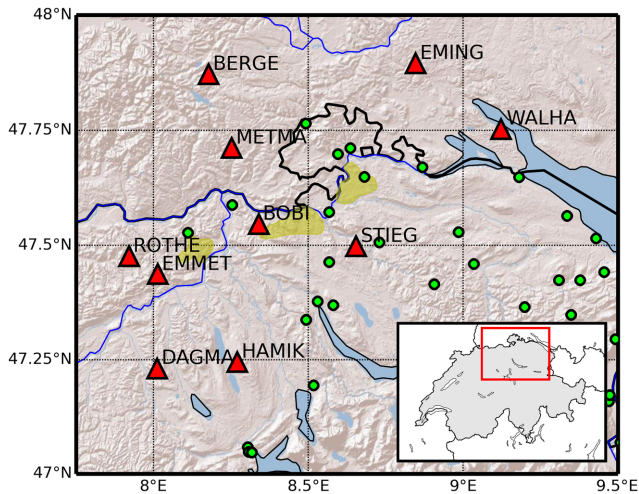


Figure 1. Location of the 10 broad-band stations of the NAGRA network (red triangles) analysed in this study. On background are also represented the stations of the Swiss networks SSMNet and SDSNet (green dots) and the areas of potential interest for nuclear waste repositories (in yellow).

Fäh 2010; Edwards *et al.* 2013). SED is also in charge of the Swiss seismic networks (the strong-motion SSMNet and the broad-band SDSNet) so that a large number of permanent stations have been characterized using passive seismic techniques, in few cases also in combination with active seismic experiments (Michel *et al.* 2014; Hobiger *et al.* 2017). For each investigated station installation, a set of best representative 1-D *S*-wave velocity profiles, derived engineering parameters (average traveltime velocities V_sZ , including V_{s30} , and quarter-wavelength parameters) and site amplification models are presently available (SED 2016).

Such site response database is useful in many ways, not only for removing the effect of local geology from recorded ground motions. For instance, this database allowed the calibration of a national ground motion rock-reference model (Poggi *et al.* 2011) for a regional GMPE (Edwards & Fäh 2013), which is now used in combination with site-specific seismic response information for the calculation of the new national seismic hazard model for Switzerland (SED 2015; Edwards *et al.* 2016; Wiemer *et al.* 2016).

The SED networks cover unevenly the Swiss territory. Some regions have been equipped more densely than others due to differences in the seismicity level or in relation to special monitoring requirements. Particular efforts have been made in the Basel region through federal and cantonal projects (18 stations characterized out of 21 currently running, see Michel *et al.* 2017), the first phase of the strong-motion renewal project (30 strong-motion stations characterized; Michel *et al.* 2014) and the assessment of rock and stiff-soil sites relevant for the development of a GMPE within the Pegasus Refinement Project (PRP, 20 stations characterized, Fäh *et al.* 2009).

Recently, the NAGRA consortium (www.nagra.ch/en), together with *swissnuclear* (www.swissnuclear.ch), has been cooperating with SED for the installation of ten new high-sensitivity seismological stations in northern Switzerland. The goal of the project is to improve the accuracy of location solutions and the detection capability of the Swiss network at sites of potential interest for future implementation of nuclear waste repositories (Fig. 1). In three cases, the seismometer was installed in a borehole, with a collocated strong motion sensor at the surface, in order to decrease the seismic noise level of the near surface.

An extensive site characterization of these sites has been carried out using state-of-art ambient vibration techniques. For the borehole

stations, moreover, the characterization was improved by combining different types of active seismic methods (*P*-*S* refraction tomography, surface wave analysis, Vertical Seismic Profiling – VSP) with ambient vibration analyses.

In this paper, we describe in detail the standard procedures we use for the characterization of the NAGRA-net stations (and more generally for the stations of the Swiss network), from survey design to final interpretation of the 1-D seismic velocity profiles and the comparison of the derived numerical amplification models with empirical observations. We show the benefits in using a well-defined protocol of analysis, which allows reproducible and consistent results that are also homogeneously represented for subsequent database storage.

As already mentioned, the NAGRA network targets the identification of small magnitude events, and for that reason the optimal choice was the installation of the seismic stations at low-noise sites, preferably on hard-rock or possibly on stiff-soil conditions.

Surface wave analysis using ambient vibration techniques has often been considered questionable at sites with rather high seismic-velocity such as in rock and stiff-soil conditions (e.g. Pileggi *et al.* 2011). This is mostly related to the mechanism of surface-wave generation, which is often assumed (although not formally required) to necessitate a sufficiently large seismic velocity contrast in order to develop surface waves of sufficient amplitude to be detected within the ambient vibration wavefield. For instance, Pileggi *et al.* (2011) performed simulations of ambient vibrations for a thin sedimentary layer over a rock layer and showed that the relative spectral power of the surface waves with respect of the full ambient vibration wavefield was low below the *S*-wave resonance frequency. However, they do not account for a realistic velocity profile at a stiff site, where a velocity gradient is expected.

So far, only few attempts have been carried out to verify the applicability of passive techniques in these special conditions (e.g. Hollender *et al.* 2017) and none of them tried to retrieve information from Love waves. Recently, the *InterPacific* project (Garofalo *et al.* 2016a)—an international benchmark study between academic and industrial partners—tried to establish more clear guidelines for the use of surface-wave based techniques, including the use of both active and passive seismic methods and for a variety of site conditions. Among others, one target of the study was the validation of surface wave methods at hard-rock conditions. For that, a mixed active-passive seismic survey was performed on top of outcropping Cretaceous limestone in the vicinity of the Cadarache research centre at Saint-Paul-lez-Durance, southeast of France. The experiment was successful in showing how close agreement could be achieved using different surface wave processing techniques with respect to an independent assessment of the local geophysical properties using direct borehole logging (Garofalo *et al.* 2016b).

In this paper, we provide additional confirmation on the reliability of using ambient vibration techniques for the seismic characterization of high-velocity sites. We analyse not only Rayleigh wave propagation, but also Love waves to better constrain the inversion of the subsoil velocity structure. Moreover, we highlight the pitfalls and limitation of the method in these conditions and provide further recommendations for the best practice.

2 NAGRA NETWORK OVERVIEW

The NAGRA network in Fig. 1 (herein NAGRA-net) consists of ten seismological stations of which nine have a sensor in free-field conditions, while one station is placed inside a tunnel at about 46 m

below the surface. Seven stations of the network are equipped with a broadband seismometer (Trillium Compact) and a high-resolution digitizer (Taurus 24Bit @200sps). Three of these stations comprise a short-period borehole sensor (Lennartz 3-D-BH 1 s) installed at variable depth and a surface force-balanced accelerometer (Kinematics Episensor). Six stations are located in Switzerland, while 4 are in Germany. We refer to Table 1 for a complete list of characteristics of the network.

From the geological point of view, the stations of the NAGRA-net are located at the border between the North Alpine Foreland Basin and the Black Forest region. The topmost bedrock units below the stations DAGMA, HAMIK, STIEG WALHA and BOBI consists of marine and fluvial deposits of Oligocene and Miocene age (Molasse), mostly sandstone and conglomerates intercalated with clay and marl layers of variable thickness and consolidation. The topmost bedrock lithology of stations ROTHE, EMMET and EM-ING is represented by Mesozoic rocks (mainly limestone and marls). Only the stations METMA and BERGE are situated on crystalline bedrock. The landform is smooth and modelled by the action of glaciers during the Pleistocene. Morainic deposits, clearly identifiable from the surface morphology, can be identified at many places surrounding the station installations.

3 SITE CHARACTERIZATION STRATEGY

Characterization of the NAGRA sites has been performed following a standardized scheme, consisting of a set of procedures (acquisition, processing and interpretation) aimed at ensuring a sufficient level of confidence on the final result before inclusion in the SED site database (SED 2016). Such scheme was originally established for the characterization of the Swiss Strong Motion network (SSMNet, Michel *et al.* 2014) and it has been subsequently refined by inclusion of additional quality-control rules based on recent experience.

The investigation protocol, schematically illustrated in Fig. 2, consists of a list of sequential steps that are conditional on the successful accomplishment of each stage. The analysis chain can be summarized as a sequence of at least four main blocks:

- I. Data gathering, survey design and field acquisition
- II. Pre-processing and preliminary quality assurance
- III. Data processing, inversion and site model build up.
- IV. Site response analysis, verification and final data storage

Each block will be discussed in detail in the following sections with a set of illustrative examples from the NAGRA site characterization. It is important to stress that, due to the strictness of the investigation protocol, several iterations might be necessary before convergence to a satisfactory result. In many cases, processing and interpretation had to be repeated in light of mismatching with empirical observations. For example, in two cases (BERGE and ROTHE) a new survey design and additional field measurements were necessary after failing of the quality analysis step.

In order to avoid subjective misinterpretations, quality analysis and verifications are always performed collectively, with the independent contribution of experts of SED not directly involved in the processing. After reporting, the review panel has the freedom to provide suggestions and/or impose modifications. In most severe cases, processing results might be rejected, and the analysis redone to provide new interpretations.

Table 1. Overview of the NAGRA-Net stations and their site properties sorted by Vs30.

Station Code	Location	Latitude	Longitude	El. (m)	Start date	Inst. type	Meas. type	EC8/ SIA261				Resonance frequencies				Traveltime average S-wave velocity					
								Surface geology	type	f_0	Type	Depth (m)	f_1	Type	Depth (m)	Vs(f ₀)	Vs10	Vs30	Vs50	Vs100	
STIEG	Oberembrach ZH, Switzerland	47.49779	8.654049	637	11.12.12	S+B	P+A	B/C	4.4	R/R	24	–	–	–	–	–	420	300	463	573	796
HAMIK	Haemikon LU, Switzerland	47.24508	8.270609	677	20.12.13	S+B	P+A	B/E	1.4	S/R	180	4.7	S/S	23	–	1110	314	488	616	835	
BOBI	Boebikon AG, Switzerland	47.5463	8.33985	570	20.12.13	S+B	P+A	B/B	1.9	R/R	140	13	S/S	6	–	1060	351	590	736	956	
EMING	Emmingen, Germany	47.89518	8.846759	619	30.07.13	S	P	B/B	1	R/R	>>200	10	S/R	6	–	>1500	306	659	932	1392	
WALHA	Wallhausen, Germany	47.7528	9.1231	419	29.07.13	S	P	B/B	0.55	R/R	>>200	13	S/R	8	–	>1500	464	766	934	1166	
EMMET	Emmethof AG, Switzerland	47.43757	8.013579	740	16.08.12	S	P	A/A	1.7	R/R	190	–	–	–	–	1300	572	801	961	1141	
DAGMA	Dagmersellen LU, Switzerland	47.23088	8.012475	560	11.04.13	S	P	A/A	0.8	R/R	>>200	–	–	–	–	>1500	729	914	1052	1264	
ROTHE	Rothenfluh BL, Switzerland	47.47612	7.92093	681	25.01.13	S	P	A/A	0.9	R/R	400	–	–	–	–	1480	666	954	1074	1203	
BERGE	Lenzkirch, Germany	47.8716	8.177979	963	01.10.12	S	P	A/A	–	–	–	–	–	–	–	–	1416	1703	1940	2205	
METMA	Mettma, Germany	47.71217	8.25262	671	28.03.13	T	A	A/A	–	–	–	–	–	–	–	–	2400	2717	2880	3015	

Notes: The depth corresponding to resonance frequencies results from the quarter-wavelength approximation and it may differ slightly from the actual depth of the interface. S: surface station; B: borehole station; T: station in tunnel; P: passive measurement; A: active seismic; R/R: rock/rock interface; S/R: sediment/rock interface; S/S: interface within sediments.

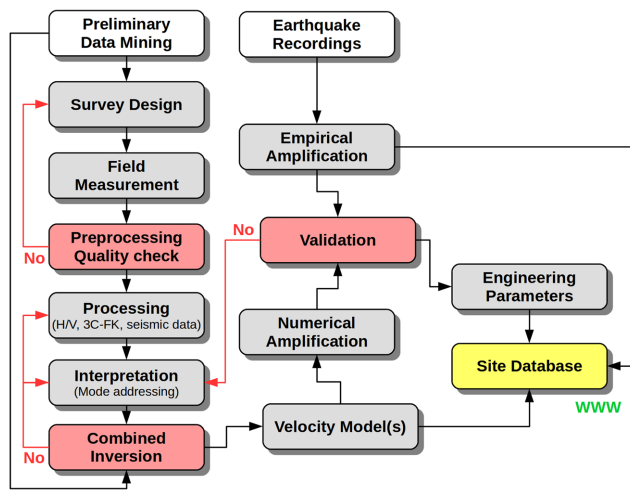


Figure 2. Schematic representation of the procedures required for the site characterization of the NAGRA seismic network.

4 SURVEY TYPE, DESIGN AND FIELD ACQUISITION

The characterization of the soil properties beneath each station of the network was mostly performed using ambient vibration (often described as passive) techniques, complemented with a set of active seismic experiments at the sites of the three borehole installations (STIEG, BOBI and HAMIK) and at the tunnel station METMA. The reason to combine active and passive seismic methods—which implied a considerable investment of resources and time—was the need for a highly accurate seismic response analysis of the sites of the borehole stations, and the necessity of validation of the ambient vibration results with independent analysis.

In this paper, we focus on describing the use of ambient vibration techniques only, although an example of the results from the combination with active surveying will be presented as well. For a comprehensive description of the type and major characteristics of the active seismic techniques used for the station characterization, we refer to Dal Moro *et al.* (2015).

For the analysis of ambient vibrations, different spectral techniques have been combined, consisting in both single station and array methods, which are listed below:

- (i) Time-frequency wavelet analysis
- (ii) Power-spectral density estimation
- (iii) Conventional horizontal to vertical spectral ratios
- (iv) Directional horizontal to vertical spectral ratios
- (v) Wavelet polarization analysis
- (vi) Three-component high-resolution f - k analysis

Results from these analyses are used to produce the final site model, in term of a set of 1-D shear-wave velocity profiles obtained by combined inversion of multicomponent surface wave information (Rayleigh and Love fundamental and higher modes). Such profiles are later used to assess the local seismic response of the station and the related uncertainty.

4.1 Acquisition equipment

Acquisition equipment for ambient vibration analysis consists of a pool of three component seismometers (Lennartz 3C with 5 s eigenperiod) and 24-bit data loggers (Quanterra Q330) sampling at 200sps. For array recordings, we used 10 to 14 stations simultane-

ously. According to our experience, a lower number of sensors potentially leads to biased results (depending on the signal quality and fulfilment of initial assumptions such as soil one-dimensionality) for the case of high-velocity sites. Ambient vibration surveys are not fully controlled experiments since the source distribution is not known. Moreover, the excitation level is low, especially at stiff sites (displacements in the range of nanometres), so it could be easily biased by very local disturbances (wind gusts, sensor-ground coupling). Although a lower number of sensors can be used theoretically (Maranò *et al.* 2014) and with particular array techniques (down to 4 and even less, as in the case of SPAC analysis, e.g. Claprod & Asten 2010), we obtained sufficiently reliable results only in few cases using reduced array geometries and f - k analysis, particularly on high-velocity sites.

Time synchronization between stations was ensured by standard GPS, while a more accurate differential GPS (Leica Viva using the *swipos* service of Swisstopo) was used to precisely locate the sensor's coordinates with a tolerance of less than 5 cm. This level of accuracy is essential for array installations of small diameter (roughly <50–100 m), while for larger arrays such requirement can be relaxed. In case of very large arrays (>~500 m), locations obtained from a standard GPS are usually sufficient. Decision criteria for array sizing on stiff soil and rock sites are discussed in the next section.

Good coupling with the ground on loose soils was assured by removing (as much as possible) the topmost weathered soil and stones digging small holes (10–20 cm deep) at the sensor's place. We experienced considerable signal degradation in all those cases where the sensors were not properly coupled to a stable ground. To facilitate the levelling of the device even in difficult ground conditions, we use triangular metal supports, which also allows a quick and precise orientation of the sensor to magnetic north.

4.2 Survey design

Before planning of the geophysical survey, geological, geotechnical and geomorphological information available for the area is collected, including any previous published study, geological maps and digital elevation models (DEMs). This is not only necessary for the proper dimensioning of the survey, but it provides also essential background information for the inversion of the geophysical data (as additional *a priori* constraints) and for the interpretation process.

In the case of NAGRA station characterization—due to the requirements of the special network—we were expecting stiff sites and therefore relatively high velocity of propagation ($\gg 400$ – 500 m s⁻¹). This implies rather long wavelengths, considering the frequency range where ambient vibration wavefields are expected to be coherent and have usable energy (roughly <15 Hz). That is two-fold: on one hand, longer wavelengths define the size of the seismic array deployment, due to the required spatial sampling. On the other hand, it also limits the maximum resolvable depth. Few empirical relations that correlates array diameter (D) with expected maximum depth resolution (Z) are available in literature. We use the approximate relation $Z = (2/3) * D$ (Wathelet *et al.* 2008). The reader should nevertheless be aware that actual resolvable depth cannot be predicted *a priori* without a proper knowledge of the subsurface structure, and even in such case, many factors can affect the result (e.g. presence of several velocity contrasts). Thus, such empirical assessment has to be considered only qualitative in all cases.

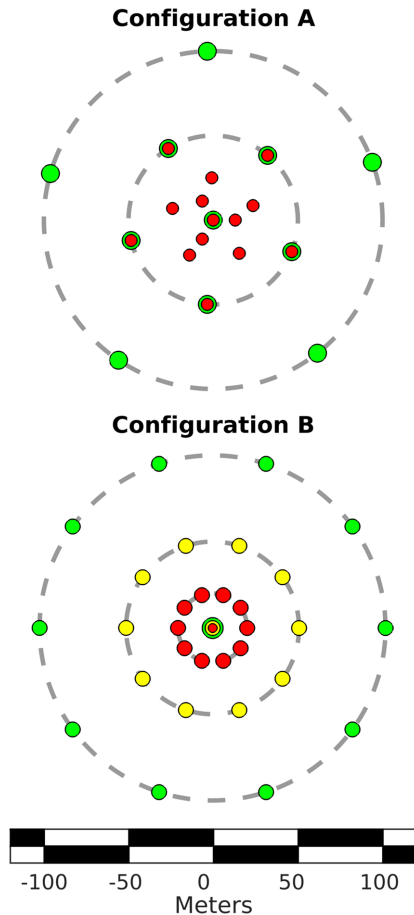


Figure 3. Representation of the two main array geometries used to acquire ambient vibrations at the NAGRA sites. Different colours represent synchronous deployments of receivers (or rings). Dashed grey lines indicate the maximum diameter of each deployment. Overlapping receiver locations are presented with multiple colours.

Geometry of the array deployment always represents a compromise between theoretical considerations and practical field limitations. Although several idealized configurations are generally possible (e.g. circular, triangular, L-shaped, square) for f - k analysis we usually prefer geometries with uniform directional response (Marano *et al.* 2014), such as circular arrays with or without internal receivers (e.g. configuration A and B in Fig. 3). These two types of circular configuration, in spite of having similar theoretical resolving capabilities, differ in many practical aspects, such as in the way they spatially sample the site. Configuration A is preferable at sites with suspected poorly uniform structure, for example nonlayered geometries, which is often the case with weathered rock conditions. Configuration B is conversely of quicker setup and allows performing several consecutive deployments in a row. Given the limited amount of recording stations and the need to resolve a broad range of wavelengths, array acquisition is nearly always performed in multiple steps, by consecutively deploying separate concentric configurations of progressively increasing size (or ‘rings’). Depending on the type of configuration used (A or B), independent rings can be partially overlapping by sharing few common sensor locations. This ensures continuity of frequency resolution between deployments.

Unfortunately, available space at a given site often imposes significant limitations to the array deployment, which in few cases ends

up with very irregular and therefore suboptimal configurations. In these cases, it is important to understand the effect of the array response (Wathelet *et al.* 2008) on the results, also in combination with concurrent sources of uncertainty, such as anisotropy in the noise source distribution and wavefield polarization effects induced by lateral inhomogeneity. These issues will be discussed later in the paper.

4.3 Field acquisition

Due to the special requirements of the high-sensitivity network, influence of buildings and anthropogenic activity seemed to be negligible at all station locations, although some disturbing signals (mainly monochromatic) have been identified during pre-processing. Duration of the recording is variable over the different sites. Although some general rules for the definition of the optimal recording length can be established, it is often beneficial to extend the measuring duration to account for some redundancy. Minimum recommended length is nonetheless controlled by the minimum frequency expected to be resolved and then by the number of wave cycles that are supposedly to be included in the analysis. Presence of transient disturbances can affect the analysis result, and therefore an increased recording duration is advisable in such cases.

We usually acquire signals for not less than 40 minutes with the smaller array configurations (<100 m), while extending to more than two hours for large geometries (>200 m).

No topographic correction has been taken into account before processing, though we tried to avoid performing measurements at places with highly irregular morphology, due to the possible implications of potential 2-D/3-D wave propagation effects.

5 AMBIENT VIBRATION ANALYSIS

5.1 Pre-processing and preliminary quality assurance

The three-component recordings of ambient vibrations have been filtered prior to analysis using a band-pass 6th order causal Butterworth filter with corners at 0.2 and 50 Hz. Although it is not a strict requirement for spectral analysis techniques, filtering is preliminary applied in order to facilitate the visual inspection of the noise traces. This procedure is useful to extract essential (although qualitative) information on the wavefield composition, such as the overall signal coherency and the density of transient disturbances affecting the recordings. For instance, measurement at site BERGE had to be repeated, as the coherency of the recorded signals was heavily degraded by disturbances due to snow melt (water flow). The issue was not apparent in the field, but evident on the recordings. Again, we point out that the absolute ambient vibration level is very low at such sites, so the measurement is extremely sensitive to the local disturbances.

To assess the energy content of the ambient vibration wavefield in the frequency band of interest, spectral analysis is then performed. Because of the stochastic nature of the ambient vibration wavefield, a statistical approach such as the estimation of the power spectral density (PSD, e.g. Fig. 4) is best suited. This approach is primarily useful to evaluate the average energy level of the recordings, but also to assess the presence of spurious large-amplitude spectral peaks (harmonic noise contributions), which might be related to human activity (machinery, pumps) from nearby sources. In few cases, single narrow-band peaks—likely of anthropogenic origin—have been identified in the spectrum and isolated. Although such signals

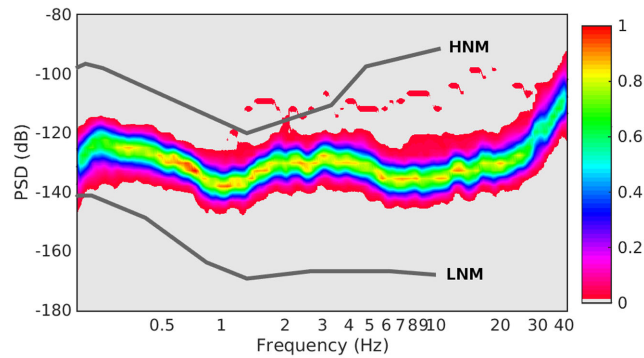


Figure 4. Example of power spectral density plot (PSD) of one hour of ambient vibration recordings (NS horizontal component) at the site EMMET. Colour scale represents signal's normalised probability. In grey lines are the minimum (LNM, low noise model) and maximum (HNM, high noise model) bounds of the USGS noise model, for comparison.

could be theoretically analysed by means of methods for active surveys, we exclude them from any interpretation, as we usually do not know their exact origin. Moreover, since the signals are typically quasi-monochromatic, they provide information only on a single frequency, what is usually not compatible with neighbouring frequencies based on ambient vibrations.

Complementary to the aforementioned statistical method, a spectral decomposition approach is more suitable to assess the stability (stationarity) of the ambient vibration wavefield over time. A wavelet based time–frequency analysis is then performed over the whole recording length, to highlight variations in the energy of the ambient-vibration wavefield and to further verify or confirm the presence of harmonic signals of anthropogenic origin (e.g. Fig. 5). In this study, wavelet decomposition is performed according to the approach proposed by Poggi *et al.* (2012b), using a tapered cosine mother wavelet with scaling coefficient (C_0) of 12.

Identified frequencies corresponding to harmonic signals of supposedly anthropogenic origin are therefore rejected from any sub-

sequent analysis and interpretation. The f – k method, in particular, is quite sensitive to the assumption of planar wave fronts, which is however not fulfilled in case of too close sources (Richart *et al.* 1970; Roberts & Asten 2008). In the near field, moreover, surface waves might not be fully developed, introducing further bias in the estimation of the phase velocity spectrum.

5.2 H/V Fourier spectral ratios

The horizontal-to-vertical (H/V) Fourier spectral ratio is a technique widely used in seismic site characterization because it permits empirical estimation of the site resonance frequencies (e.g. Nogoshi & Igarashi 1971; Nakamura 1989; Haghshenas *et al.* 2008 and references therein) through identification of maxima in the H/V function. Direct inversion of the spectral ratio curves is also possible and often used to infer key characteristics of the soil structure, such as resolving large velocity contrasts at depth (e.g. Parolai *et al.* 2005; Asten *et al.* 2014; Manea *et al.* 2016). Different approaches have been proposed in the literature, each based on different interpretation of the phenomenon and relying on specific base assumptions. Horike (1985) hypothesizes that surface waves are the most significant contribution to the ambient vibration wavefield at sites with clear 1-D resonance phenomena. Based on that, Arai & Tokimatsu (2004, 2005) proposed a method, subsequently improved by Picozzi & Albarello (2007), to mimic the full shape of the H/V function by analytical solution of the full surface wave field, including higher modes. Their approach, however, relies on *a priori* definition of weakly constrainable quantities, such as the spatial distribution of noise sources and a fixed proportion between Love and Rayleigh wave energy. Such assumptions might not be necessarily fulfilled at all sites (Hayashi *et al.* 2011) and over different frequency bands. Fäh *et al.* (2001, 2003) observed that Rayleigh wave contribution is nonetheless dominant and rather stable at the frequencies of the right flank of the H/V first maximum. In those studies, it was claimed that inverting only this portion of the curve could help reducing the sensitivity to energy partitioning assumptions between surface wave types, which can then be accounted for by scaling the H/V

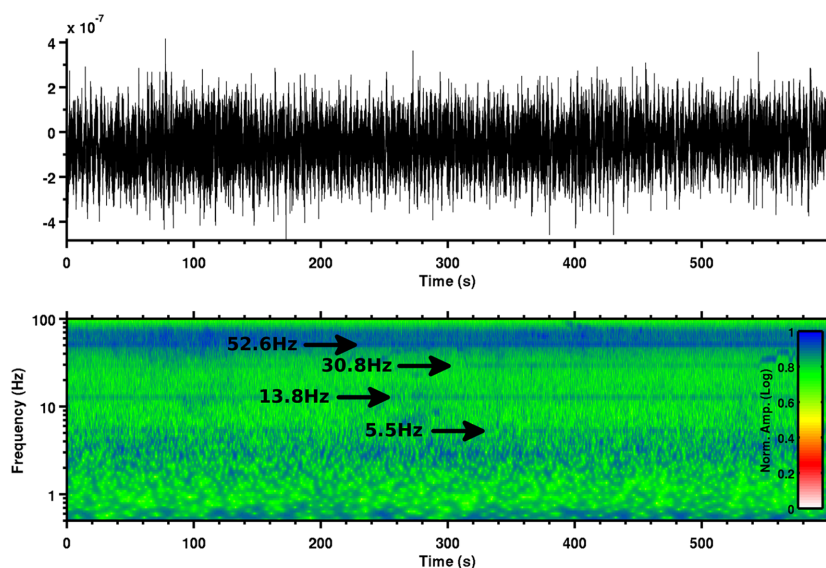


Figure 5. Spectrogram of 600 s of ambient vibration recordings at the station DAGMA (in this example the vertical component). For the analysis, the wavelet transform is used with a tapered cosine mother wavelet (Poggi *et al.* 2012b). Some harmonic disturbances (from a nearby farm) are visible on the whole spectrogram. Affected frequencies have been rejected from following interpretations.

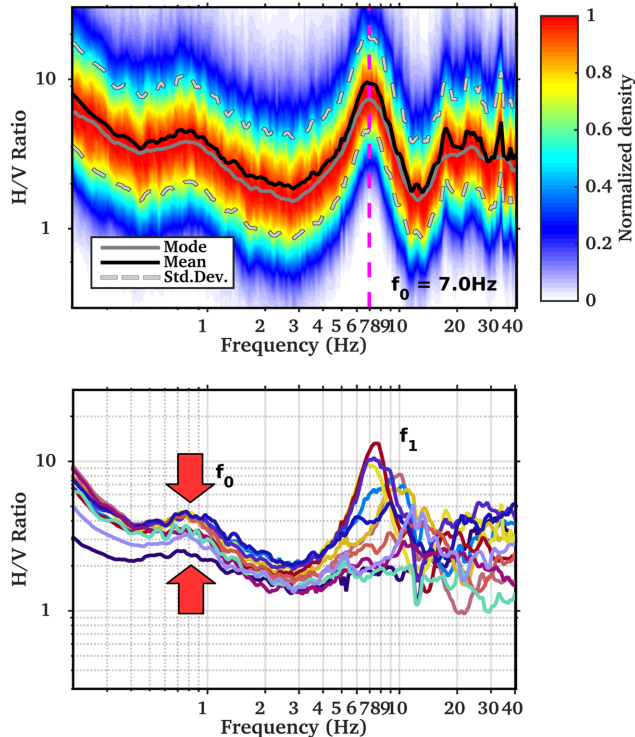


Figure 6. Example of ambient vibration H/V Fourier spectral ratios performed at the site DAGMA. The largest high frequency peak has been initially erroneously interpreted as the site (f_0) at the central station of the array (top panel; colour scale representing the signal's normalised probability). Comparing H/V curves from all stations (bottom panel), the presence of a stable low-frequency peak of moderate amplitude (the actual f_0) is more evident, while the high-frequency peak (f_1) is irregularly varying over the area (even disappearing at some measuring locations) and it reflects the heterogeneity of the topmost sediment cover (probably colluvium or weathering material of lower-velocity).

amplitude by a just constant factor. Similarly, Ikeda *et al.* (2013) showed that using zero-lag cross-correlation could help to further reduce sensitivity on H/V amplitude mismatching. For the station of the NAGRA network, we used the right flank of the observed H/V curves assumed representative of Rayleigh wave ellipticity to invert for the soil properties, jointly with dispersion curves from three-component f - k analysis. Such procedure will be examined in more detail in the following sections.

In our site characterization procedure, H/V spectral ratios are also used as tool for preliminary quality check. By comparing spectral ratio curves at all stations of the array installation it is possible to map the variability of the soil response along the investigated area; this is useful to confirm the fulfilment of the 1-D structure assumption, which is an important requirement for the application of f - k methods, as it will be discussed in the next sections. A very similar H/V across the array can be considered as necessary (but not sufficient) condition for application of 1-D methods. At the site DAGMA, for example, H/V analysis allowed identifying the disturbing presence of a spatially-variable shallow colluvium layer, responsible for the large high-frequency maximum in H/V ratios irregularly distributed (or even missing in some locations) over the measuring area. This site variability would not have been evident by the analysis of the just one station (Fig. 6 top, central sensor of the array), but only through the evaluation of all avail-

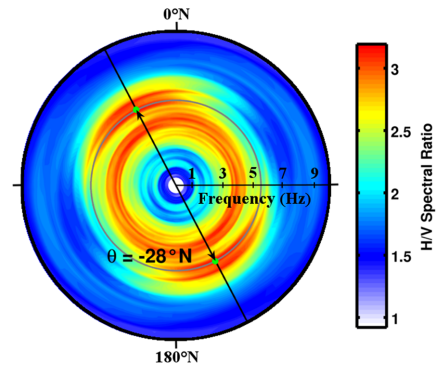


Figure 7. Example of directional H/V spectral ratio analysis at the NAGRA station STIEG. The fundamental frequency (as well as the second H/V peak) shows a certain directionality along NNW–SSE, which was subsequently interpreted as a moderate effect of the topography slope, dipping toward the same direction. Such effect, although evident from the analysis, did not bias the results of the subsequent site characterisation procedures.

able measuring locations (Fig. 6, bottom). Moreover, by removing those stations more heavily affected by sediment resonance, a better estimate of the bedrock velocity structure was then achieved with array analysis, despite having reduced the number of spatial samples.

5.3 Directional analysis

The analysis of the directional characteristics of the wavefield is useful to reveal potential asymmetries in the source distribution around the measuring location or the influence of heterogeneities in the soil structure, such as buried 2-D/3-D geometries (Ermer *et al.* 2014) or effects observed at terrain irregularities (Burjanek *et al.* 2014). This is an important step to assure quality and reliability of the subsequent analysis results, and is also essential to properly setup the working assumptions needed for the subsequent site-response analysis.

At first, one can analyse the directionality of the ground motion at a single site. The easiest way to perform this kind of analysis is through the use of directional H/V spectral ratios, which can be produced by computing the spectral ratios on a direction-dependent combination of the two horizontal components (e.g. Matsushima *et al.* 2014). By progressively varying the projection direction to cover all possible azimuths, it is then possible to reveal the presence of irregularities in amplitude and frequency of the fundamental peak, as well as any directional dependency of the energy distribution over different frequency bands (e.g. Fig. 7). If a strong directional dependence is found by the analysis, it is generally recommended to carry out further investigations on a wider area to properly address the origin of the wavefield polarization, which can be ambiguously induced by either a spatially asymmetrical source distribution or by local geometrical effects. This kind of ambiguity can be unravelled by combination of wavefield polarization analysis (e.g. using the wavelet-transform based method of Burjanek *et al.* 2010) and noise-source azimuth mapping. The three-component frequency-wavenumber analysis can be used for this purpose, as it will be discussed more in detail in the next section. Finally, if the influence of a relevant geometrical effect is confirmed, the site characterisation should not proceed with the standard workflow, but ad-hoc analysis might be carried out instead (e.g. Roten & Fäh 2007; Claprod *et al.* 2011; Bergamo *et al.* 2012).

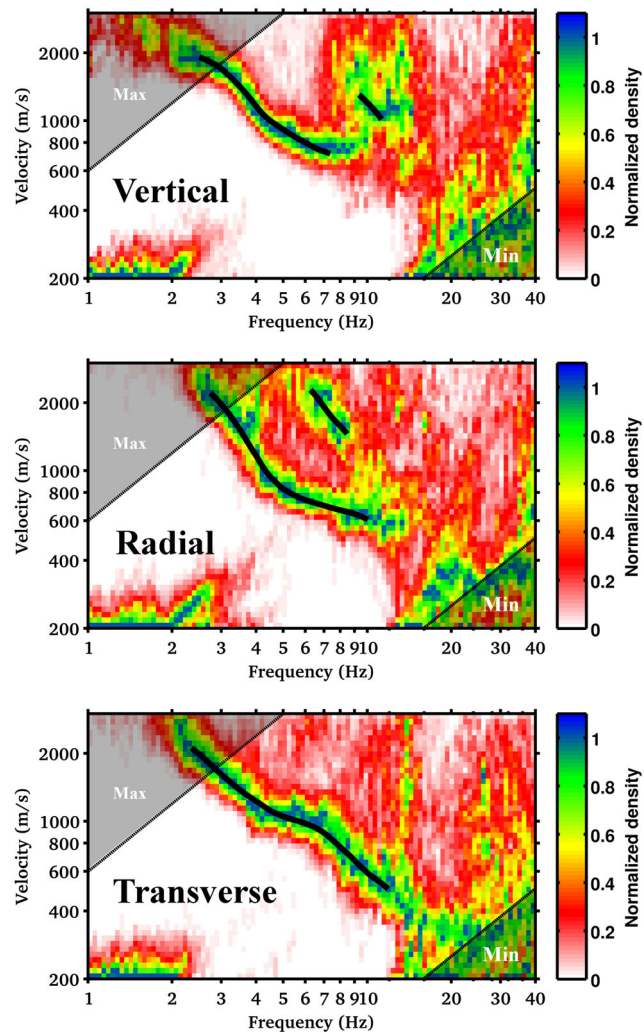


Figure 8. Normalized density distribution of surface wave signals identified using f - k analysis separately for the three components of motion (station BOBI). From top to bottom: Rayleigh (vertical and radial) and Love (transversal) wave dispersion pattern. Interpreted dispersion curves are marked in black, while grey regions indicate the resolution limits of the array.

5.4 Three-component f - k analysis

The frequency-wavenumber analysis is a spectral technique based on seismic array recordings that allows retrieving direction and dispersion characteristics of the surface waves (Asten & Henstridge 1984; Okada 2003). We apply this technique to three-component ambient vibration recordings using a modification of the high-resolution method of Capon (1969) as described in Poggi & Fäh (2010). Using all the three-components of motion gives the possibility to retrieve information about the propagation of the Rayleigh waves (*vertical* and *radial* processing direction) as well as of the Love waves (*transverse* direction). The SED uses nowadays routinely this approach for the seismic characterization of Swiss sites (Michel *et al.* 2014), including local microzonation studies (Fäh *et al.* 2008; Poggi *et al.* 2012c). All NAGRA station sites (with the only exception of METMA, because of site inaccessibility) have been investigated this way (e.g. Fig. 8).

Using three-component f - k analysis offers multiple advantages. Love waves are only affected by the shear modulus and density of the soil and therefore their use provides a more efficient constraint

for the inversion of the V_s profile than simply using Rayleigh wave from vertical component (so far the most widespread approach). Moreover, incompatibility of the Rayleigh and Love inversion results when using an isotropic dispersion solver may indicate soil anisotropy, either due to geometry (layering, fracturing) or composition. Furthermore, the combined analysis limits the possibility for errors when assigning the modes.

As for the case of the previous methods, ambient vibrations are analysed statistically by subdividing the seismic recordings into several consecutive blocks of shorter length. f - k analysis is then performed for each signal window separately, and the result from all blocks finally averaged. This is primarily done to stabilize the processing results (see Poggi & Fäh 2010 for further detail on signal covariance matrix stacking), but it is also useful to explore statistical characteristics of the wavefield. For example, a side product of the 3C f - k processing is the azimuth of each identified source generating a surface wave signal. Representing the distribution of these sources on a polar plot gives immediate perception of any potential asymmetry in the source distribution. As we were mentioning in the previous section, this is advantageous in combination with single station directional analysis to confirm/reject the occurrence of geometrical effects and consequently to verify the fulfilment of the one-dimensionality assumption for the site. Azimuthal distribution of sources can be mapped separately for different frequency ranges and for each component of motion (e.g. Fig. 9), not always necessarily matching.

Nonetheless, such statistical approach to f - k analysis is also beneficial for surface wave dispersion evaluation. Low energy portions of fundamental as well as higher modes are better resolved. Exploration of uncertainty is possible through the direct analysis of the f - k signal histogram.

6 INVERSION OF MULTIPLE DATA SETS

The surface wave dispersion curves (Rayleigh and Love) obtained from the array analysis of the ambient vibrations are used to estimate the 1-D velocity structure of the site (mainly S -wave velocity as function of depth, and to a lesser extend the P -wave velocity, due to the lower sensitivity) by solution of an inverse problem. Such analysis is performed using the software *Dinver* (www.geopsy.org), which implements a direct search approach based on a conditional version of the neighbourhood algorithm (Sambridge 1999; Wathelet 2008).

6.1 Handling multiple data sets

Combined inversion of multiple data sets is often not trivial, due to the different sensitivity of each data set to the model parameters. Multiple data sets are a combination of homogeneous and inhomogeneous data. We describe as inhomogeneous data the curves from different modes (fundamental, first higher etc.), ground motion component (Love and Rayleigh) or physical quantity (dispersion, ellipticity). Portions of the same curve (e.g. the fundamental Rayleigh) but in different frequency bands and/or from different processing technique (active or passive) are considered homogeneous data.

Due to their different sensitivity, different significance should be given to each data set when a joint misfit function is calculated. In the easiest way, this can be done by weighted sum of separated error functions. The major problem is clearly assignment of weights. We use a trial and error approach, consisting in progressive adjustment

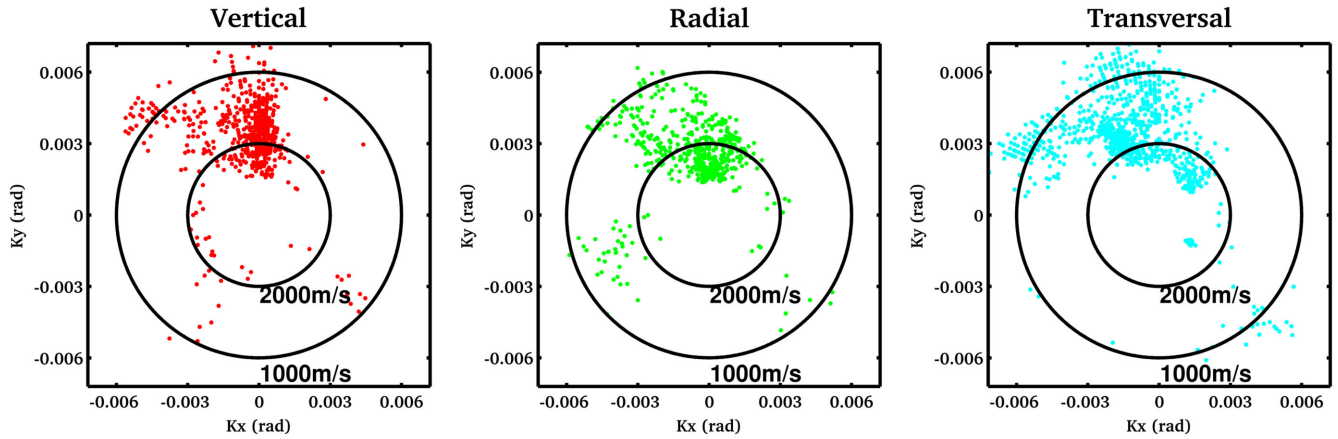


Figure 9. Azimuthal distribution of noise sources in the frequency range 4–8 Hz obtained from three-component f – k analysis at station WALHA. The source distribution is strongly directional on all components of motion. This condition does not bias the quality of the result, but might limit the generalization of the inversion result to entire site.

of the relative importance assigned to each data set in relation to fit and characteristics of the output model.

Major problems arise when multiple data sets appear incompatible and cannot be jointly inverted. This might be the case when too simplified assumptions are used (e.g. soil isotropy and one-dimensionality), but can also be the case of data affected by large errors. This second case is more common on high velocity sites, where large uncertainties are due to less efficient generation of surface waves in case of limited velocity contrasts. For the characterisation of the NAGRA network, if no strong argument exists otherwise, we usually assigned more weight (larger significance) to surface wave fundamental modes, and in particular to the Love component, which estimate is often (although not always) reliable, particularly at high frequencies. Radial component of Rayleigh waves, on the contrary, is frequently regarded as too uncertain and is used with very low weighting for the inversion.

6.2 Mode addressing and interpretation

In few cases, interpretation of surface wave dispersion might be ambiguous, as the simple analysis of f – k results might not be sufficient to uniquely sort the retrieved modal pattern. Providing a spectrum of plausible interpretations compatible with observed data generally solves the issue. The different interpretations are first inverted separately and inversion results are subsequently compared in term of fitting residuals and output velocity structure. Models with too large residuals (practically when a reasonable fit cannot be obtained) or providing unrealistic velocity profiles for the expected site conditions are rejected. The use of multiple data sets and *a priori* information sensibly reduces the possibility of erroneous interpretations. Fig. 10 is a good example of such case. Here, Rayleigh dispersion between 6 and 19 Hz could have been interpreted either as fundamental or as first higher model. The joint use of Love wave dispersion confirmed the first interpretation, but also including a modal jump at about 7 Hz.

6.3 Using Rayleigh wave ellipticity

The frequency corresponding to the first peak of the H/V spectral ratio curves has been used at nearly all sites as a constraint to resolve the depth of the deepest resolvable velocity contrast of the profile, usually the hard-rock basement interface. Although such

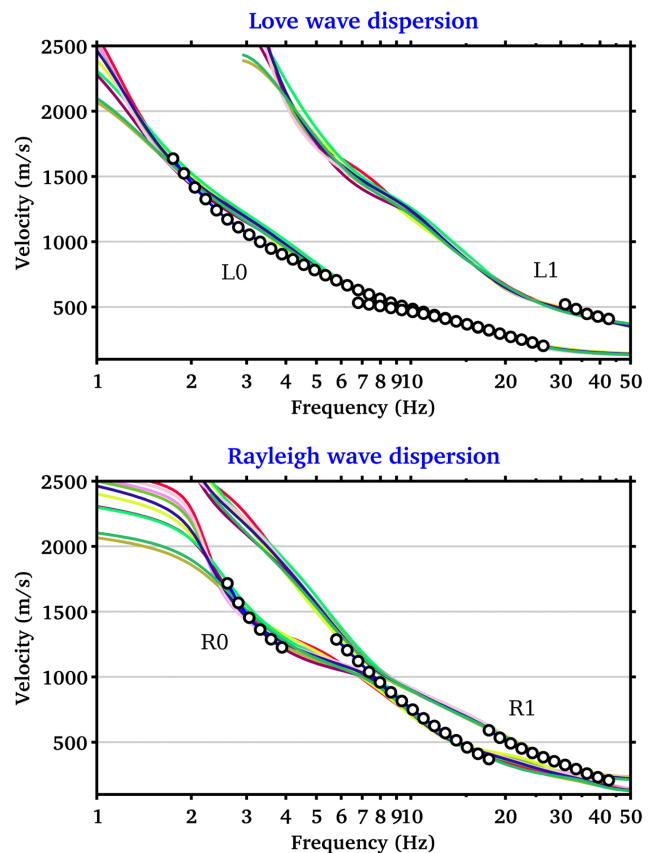


Figure 10. Example of fitting observed Love and Rayleigh dispersion curves from three-component f – k analysis (black dots) with a theoretical model (solid coloured lines) at station HAMIK. The high frequency part (>25 Hz) is derived from combined use of active seismic surface wave analysis (see Dal Moro *et al.* 2015 for details).

peak is considered a reliable proxy for the fundamental frequency of resonance of SH-waves, we model it during the inversion as the largest peak of the Rayleigh wave ellipticity function (fundamental mode). This is in agreement with the assumption of a dominant contribution of Rayleigh waves to the ambient vibration wavefield (see Bonnefoy-Claudet *et al.* 2006 for a literature review). In few cases, the right flank of the H/V first maximum has been inverted

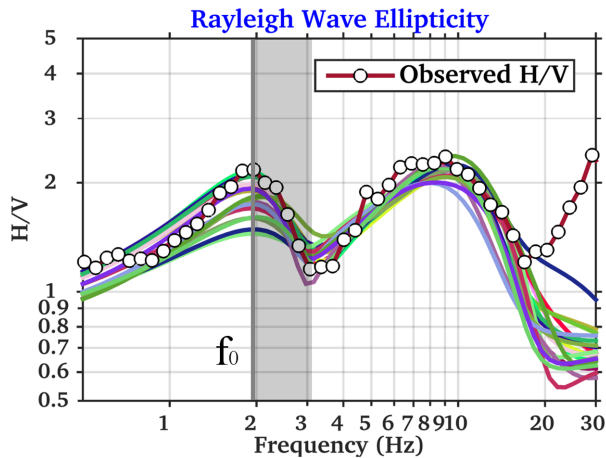


Figure 11. Example of fitting observed H/V spectral ratio (scaled by square root of two) with theoretical Rayleigh ellipticity functions at station BOBI. In light grey is the frequency region actually used for the inversion (the right flank of the ellipticity first maximum), while the assumed fundamental frequency of resonance (f_0) is indicated with grey solid line.

as a portion of the Rayleigh wave ellipticity, after normalization by square root of two to account for contribution of Love waves (Fäh *et al.* 2001). For several sites, a good matching between observed H/V and Rayleigh ellipticity was found also in frequency bands not directly used as constraint (Fig. 11). This might be evidence that on stiff soils and rock sites the contribution of Rayleigh waves to the noise wavefield is important.

6.4 Model parameterization

To parameterize the velocity model, two different although complementary strategies are used in a two-step approach, with the goal of reducing the model complexity and consequently the non-uniqueness of the inversion problem. Such technique shares some similarities with the method proposed by Renalier *et al.* (2010).

In our approach, a first parameterization scheme is implemented by setting up a layered model with fixed interface depths (or constant layer thickness). In such a case, the free inversion parameters are just seismic velocities (P and S) and densities of each layer, while layer's thickness is *a priori* imposed to be increasing with depth by geometric-like progression (in relation to the decreasing resolving power of surface waves). To further reduce the variability of the solution, search space for the free parameters is bounded between maximum and minimum values, chosen in agreement with the geology expected for the site. However, when poor or no local information is available, few explorative inversion trials might be initially necessary to setup reasonable search bounds. An increase of the seismic velocities with depth is usually assumed as a conditional search constraint, unless there is *a priori* information about potential low-velocity zone. Moreover, P - and S -wave velocity are allowed to vary within an admissible Poisson ratio range, which for the case of (weathered) rock sites is assumed between 0.2 and 0.4. Anelastic parameters (quality factors, Q_p – Q_s) are presently not considered, but this option will be explored in the future.

Although the *fixed-depth* parameterisation scheme considerably reduces the non-uniqueness of the inversion problem by decreasing the size of the parameter search space, it has the limit to potentially misplace layer interfaces with sharp velocity contrasts, which might be relevant for predicting the seismic response of the site. The issue

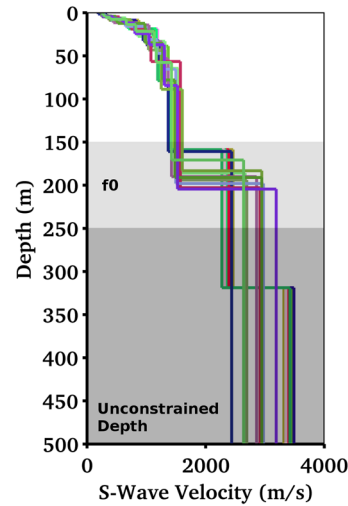


Figure 12. Best-fitting velocity profiles from a series of independent inversion runs by joint analysis of Love and Rayleigh dispersion curves and site f_0 (here for station BOBI). The profiles are progressively less constrained for increasing depth, as confirmed by progressive spread of the velocity models.

is then solved by introducing a second *free-depth* layer parameterisation scheme. Such complementary approach has now resolution on the layer geometry, but is conversely affected by a lower sensitivity of the seismic velocities. These are nonetheless bounded by the results of the first inversion step.

In case of rock and stiff soil site, velocity structure is typically gradient-like. Layer interfaces with a significant velocity contrast might still be present, particularly closer to the surface; here weathering, fracturing and the presence of a topmost ground layer can sensibly reduce the elastic moduli of the material. In these conditions, the combined use of the two complementary parameterisation schemes has proved successful to describe epistemic uncertainties, and joint analysis using both strategies is key to better converge to a reliable velocity estimate.

6.5 Model uncertainty exploration

To explore the variability of the inversion results, several inversion tests (or *runs*) are performed for each interpretation and parameterisation trial (Fig. 12). Given the stochastic nature of the optimization algorithm being used, multiple runs are useful to minimize the effects of a possible unfavourable initial randomization of the parameter space, but also to explore the uncertainty of the modelling assumptions, by performing a-posteriori statistic on derived engineering quantities (e.g. soil proxies, amplification functions), which will be introduced in the next section.

It has to be noticed that, if each considered inversion run is performed starting from a common inversion scheme (same initial assumptions, model parameterization and data interpretation) the resulting uncertainty is merely representing the aleatory component of the algorithm used for optimization. However, if results from different inversion strategies are combined into the analysis (e.g. using different *a priori* information or different mode addressing), also the epistemic (knowledge-related) component of model uncertainty is explored.

The selected velocity models from independent runs are then stored in a database located in a centralized ad-hoc server, together with seismic recordings, raw and processed data and the

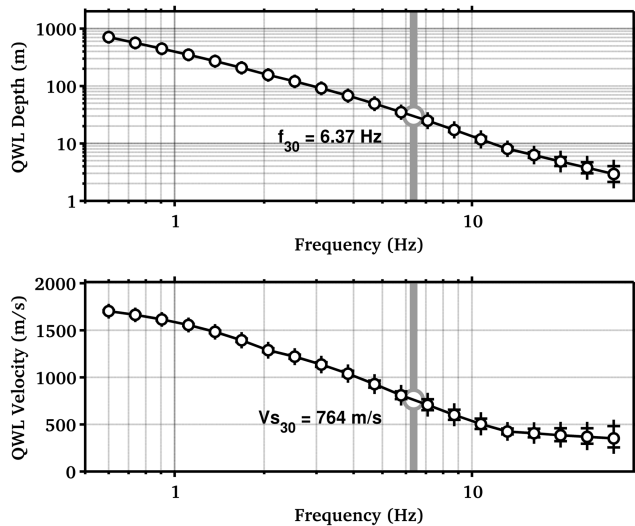


Figure 13. Example of use of the quarter-wavelength approximation at the site WAHLA. On bottom the Qwl average velocity function versus frequency, while on top corresponding averaging depths. The V_{s30} is indicated with grey bar for comparison, and corresponds to a Qwl-frequency of about 6.4 Hz.

documentation. Depending on the number of alternative hypotheses explored in the analysis of a site, the number of stored profiles might range from 16 to 40. Storage of the profiles is presently done without ranking, which means equal significance assigned to each model. A ranking approach could only be established with a framework for uncertainty quantification independent of inversion targets and parameterization schemes, presently not available. From the database, then, data are directly retrievable as files on a shared file-system, API's or through an interactive web-frontend.

7 ENGINEERING PARAMETERS

The set of best-fitting velocity profiles from each separated inversion run is finally used to compute various engineering soil proxies (e.g. average velocities for geotechnical classification and ground motion analysis) and numerical amplification models.

Among different soil proxies we primarily compute mean velocities using the standard traveltime averaging over different investigation depths (V_{sZ} , including the popular V_{s30}) and by means of the quarter-wavelength approximation (Qwl- V_s , Joyner *et al.* 1981). While the former is a standard approach used for ground-type classification in building codes (e.g. CEN 2004) and in GMPEs (e.g. Akkar *et al.* 2014), the Qwl approximation is a more sophisticated method which allows investigating the sensitivity of the seismic wavefield to the structural characteristics of the site for an arbitrary given set of frequencies (e.g. see Fig. 13). Furthermore, we have successfully used this method to empirically predict site-specific ground motion (Edwards *et al.* 2011; Poggi *et al.* 2012a, 2013) and seismic amplification factors (Poggi *et al.* 2011).

8 AMPLIFICATION MODELS AND VALIDATION

Numerical amplification functions are computed using two different strategies: the S -wave transfer function (as formalised in Knopoff

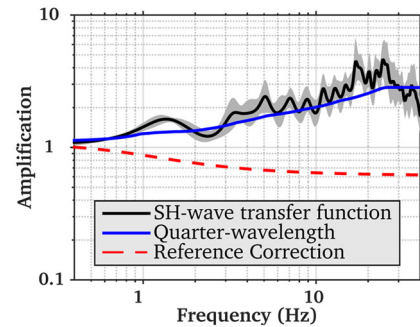


Figure 14. Comparison between mean SH-transfer function and Quarter-Wavelength amplification computed from the selected velocity profiles at site HAMIK. Both models are corrected for the Swiss (rock) reference conditions (red dashed line) using the procedure described in Edwards *et al.* (2013). Standard deviation of the SH-transfer function is shown with a grey area.

1964) and the quarter-wavelength approximation (Boore & Joyner 1997). The first method is theoretically rigorous and provides the exact representation of the seismic resonance characteristics of the site. The second method is coarser, as it can only provide a first order estimation of the maximum amplification related to average velocity contrast between uppermost layers and underlying bedrock, not modelling resonances. This technique has nevertheless the advantage of being less influenced by artificial discretisation of the profiles in a limited number of layers, which might lead to spurious resonance amplification peaks on the spectrum, not necessarily representing reality. Moreover, it is particularly relevant for rock sites where resonances are less likely. In case of rock or stiff-soil sites, the two methods are therefore to be considered complementary and should be analysed together (Fig. 14).

Numerical amplification models are finally compared with empirical amplification functions obtained for each station of the network from spectral modelling of low-magnitude earthquakes, as described in Edwards *et al.* (2013) and Michel *et al.* (2014). It has to be noted that numerical and empirical amplification models are all commonly referenced to the Swiss rock reference velocity profile, as defined in Poggi *et al.* (2011), following the procedure described in Edwards *et al.* (2013).

If a good matching is obtained from the comparison, that is the presence of resonance peaks at the same frequencies and comparable levels of amplification, a site model is finally archived into the SED database (SED 2016). If matching is not satisfactory, however, the analysis is performed again, checking for processing errors or exploring alternative interpretations. In some cases, however, a match cannot simply be obtained. This is the case for example when strong 2-D/3-D resonance effects are affecting the observed ground motion, but cannot be captured by standard site investigations. If such a case is identified, results are eventually stored, including a note on the occurrence of these phenomena in the final report. On the other side, empirical amplification functions can also be biased, for example in case of limited availability of earthquake recordings at the station or by the effect of a poorly constrained site attenuation, which affect the fitting of the spectrum.

9 INTERPRETATION OF THE RESULTS AND DISCUSSION

The procedure presented in this paper resulted in shear-wave velocity profiles for nine stiff sites (Fig. 15). In general, profiles are

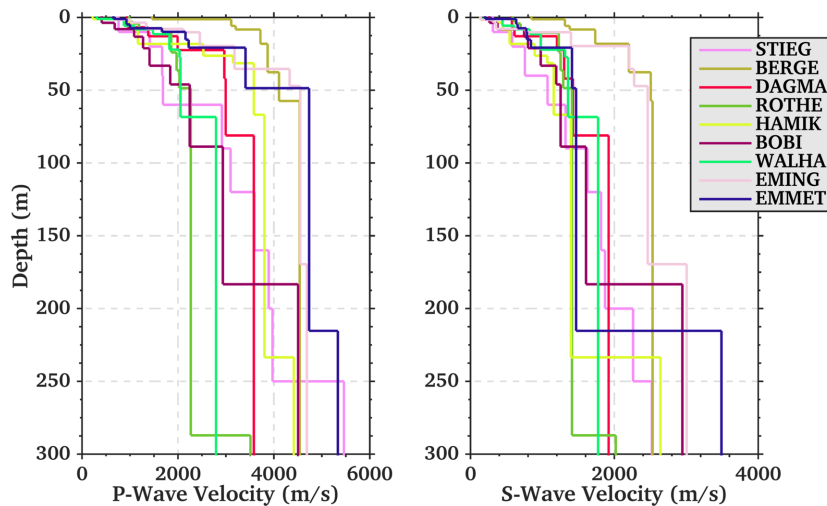


Figure 15. Summary of P - and S -wave profiles of all NAGRA stations investigated using ambient vibration analysis (for simplicity, only the best fitting model is presented for each site). While V_s profiles are typically well resolved by the combined inversion of Love and Rayleigh data sets, V_p estimates are still affected by a rather large uncertainty (see details in the text).

characterized by gradual increase of shear wave velocity with depth. S -wave velocities are generally well resolved in the upper 40–60 m, with uncertainty usually less than about ± 5 –15 per cent. Resolution gradually decreases with depth, with errors typically around 15–30 per cent and up to 50 per cent in the lowermost constrained layers of the profile. Resolution of V_p is poorer for inversion of surface wave data (Xia *et al.* 1999) and for the high velocity sites in this data set uncertainty is typically a factor 2 to 3 larger than for V_s estimates. Nevertheless, the actual uncertainty range for V_p is difficult to quantify and could be larger, particularly at those depths constrained by just Rayleigh ellipticity information.

Sites BERGE and EMING show clearly higher velocities ($>2500 \text{ m s}^{-1}$) in the intermediate depths (20–100 m) that can be explained by the geology. It should be noticed that Vs30 (Table 1) is not mapping this feature due to variable low velocity layers near the surface. BERGE is located within a geological unit of the Black Forest area, which mostly consists in granite and gneiss of different metamorphic degree. EMING sits on bedded limestone and cemented marls of Jurassic age. On the contrary, sites BOBI, DAGMA, HAMIK, STIEG, and WALHA are located within the Swiss Molasse basin on marls and sandstones of Tertiary age, what explains reduced seismic velocities. Nevertheless, ROTHE and EMMET are located in the Jura massif, on limestone and marls of Jurassic and Triassic age, respectively, and also show lower seismic velocities. They are similar to EMING in terms of genesis but suffered deformation during the uplift of the Jura range, which may explain these lower values. This shows once more that geology alone is not enough to accurately assess its effect on ground motion and that local measurements are necessary to derive the velocity profile. As expected, Vs30 is lower at borehole sites. The response of these stations is studied in more details in the electronic supplement.

The resonance frequency analysis (Table 1) reveals that a typical sediment/rock interface is rarely observed. It can be seen at site HAMIK, where rather deep sediments are found (down to about 120 m from the borehole log), or at those sites with a shallow quaternary soil cover, such as WALHA and EMING. At several stations (e.g. DAGMA, ROTHE), the high frequency peak observed on the array measurements is not visible on the recordings from the permanent station. In contrast, several seismic interfaces within

rock layers are evident from the H/V analysis. It concerns lithological boundaries within the Molasse basin (STIEG, DAGMA) but also deeper interfaces, not resolvable by standard characterization techniques and hardly inferred from surface geology.

The synthetic 1-D response based on these profiles is generally—although not always—in a good agreement with the observed amplification functions (Fig. 16, see Edwards *et al.* 2013 and Michel *et al.* 2017 for a comprehensive discussion on the spectral modelling method to obtain empirical elastic and anelastic amplification models). This justifies the assumption of horizontally layered media made during the site characterization procedure. Conversely, derived velocity profiles could be used to identify problems in the empirical amplification functions. For example, in case of station EMING, the total empirical site amplification including near surface anelastic attenuation (dashed black line, Fig. 16) is in a good agreement with the synthetic response while the empirical elastic amplification is not. This is likely caused by the trade-off between the anelastic attenuation (κ , Anderson & Hough 1984) and elastic amplification during spectral modelling (i.e. the elastic amplification was reproduced by low attenuation) as explained by Michel *et al.* (2017). Station HAMIK and BOBI show a similar but less pronounced effect, with a clear underestimation of the elastic spectrum at high frequencies. Station BERGE presents a low attenuation as well, however, since the elastic amplification fits well the response based on the velocity profile, the low κ value can be considered as reasonable in this case. Therefore, the procedure described in this paper could potentially improve the κ estimates for the rock- and stiff-soil sites that are generally very uncertain (Edwards *et al.* 2015). BERGE and EMING show the lowest attenuation, related to their high velocities at intermediate depth. Since κ is relative to the average Swiss conditions, it results here in a negative attenuation (anelastic spectrum larger than the elastic one). BERGE is also the site with the strongest de-amplification (about 50 per cent around 1 Hz) compared to the Swiss reference. Stations like ROTHE or EMMET show clear amplification peaks (factor of about 2) at their fundamental frequency between 1 and 2 Hz. At higher frequencies, stations with low-velocity subsurface show even stronger amplifications up to a factor of 3. This results in differences of factors up to 4 for sites considered as rock (soil type A) for Eurocode 8 (Table 1; CEN 2004) (e.g. between BERGE

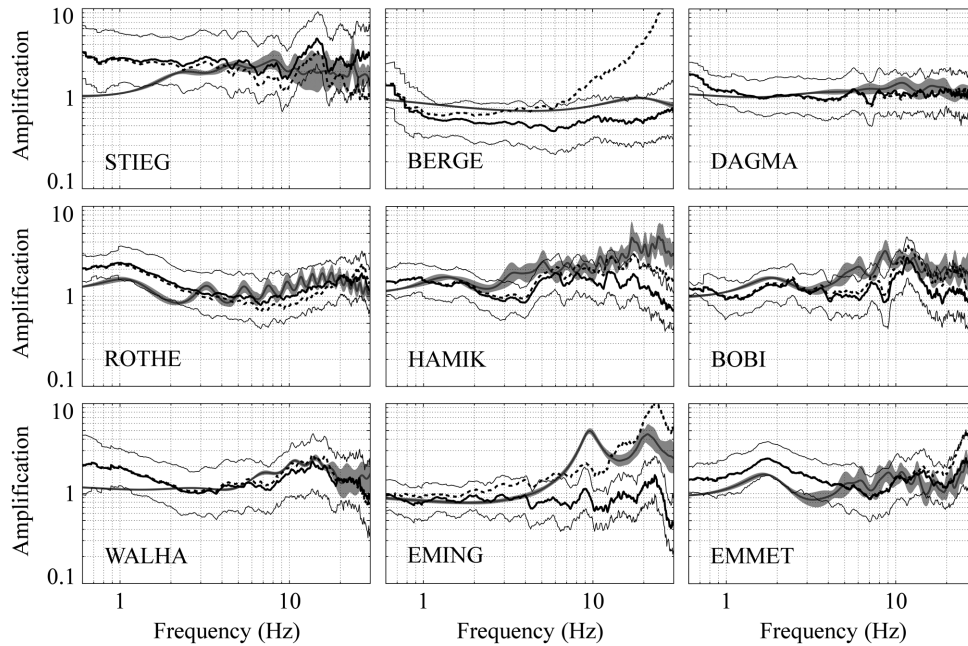


Figure 16. Comparison between elastic empirical (black solid line), empirical including kappa (black dashed line) and numerical (dark grey line) amplification functions at all NAGRA station sites. Simulations are computed using all best-fitting models from each independent inversion run. Standard deviation of the elastic empirical (light grey line) and numerical (light grey area) functions are also provided for comparison. We refer to Edwards *et al.* (2013) and Michel *et al.* (2014) for a comprehensive description of the spectral fitting method to obtain empirical amplification models.

and EMMET or ROTHE). Conversely, amplitude of the empirical amplification functions is not well-constrained at long-periods (roughly below 0.8–1 Hz, e.g. BERGE and DAGMA), as it might be affected by the combined effect of deep site effects, as revealed by the H/V analysis, and intrinsic processing limitations. Therefore, a comparison is not conclusive in this frequency range.

10 CONCLUSIONS

The analysis of surface waves composing ambient vibrations was shown to be useful even for stiff rock sites, providing well-constrained information on shear-wave velocity down to few hundred meters. We underline that this is achieved by joint inversion of multimode dispersion (Love and Rayleigh) and ellipticity curves (including f_0). Especially the latter allows for reaching greater depths, which are otherwise hardly resolvable by arrays of limited extension. We could observe the dispersion of Love waves in the ambient wavefield even in such stiff sites, and therefore better constrain the inversion of the uppermost shear-wave velocity structure, which was not tried by previous authors working on this type of sites.

The use of a well-established protocol for the analysis showed up to be crucial to avoid processing mistakes otherwise not easily recognizable and to make processing results comparable among stations. This is essential for populating the SED site-characterisation database with homogeneously represented velocity profiles. In particular, we highlight the need to store and analyse populations of velocity profiles for each characterised site, in contrast to the nowadays-standard practice where a best-representative velocity model is usually considered. We recommend considering whenever possible a broader spectrum of models, particularly when Monte Carlo-like approaches for the inversion are used, to represent the uncertainty of the input data and the stochastic variability of the inversion result. Moreover, to face the non-uniqueness of surface wave inversion solution, we found particularly useful the combined use

of different soil parameterisation strategies, such as the free- and fix-layer approaches.

The obtained velocity profiles, although correlated to the geology, could not have been retrieved quantitatively based on this sole criterion. Amplifications up to a factor of 4 have been observed between these ‘rock sites’, which cannot be modelled using the Vs30 site proxy and the widespread half-space simplification. This impact is therefore critical for the seismic hazard at sensitive facilities such as nuclear waste repositories, nuclear power plants or dams, generally built on stiff sites. It is therefore evident that accurate modelling needs accurate site-specific velocity profiles, accounting for velocity gradients with depth and any rock-rock seismic impedance discontinuity potentially capable to generate amplification. The investigated rock sites have a surface layer characterized by weathering. This affects the high-frequency response being very site-specific.

The retrieved velocity profiles could potentially constrain regional velocity models, which could then be used for waveform inversions (e.g. moment tensor inversions). For a long-term accessibility of these results, site characterization data of SED seismic stations can be retrieved through a web-interface (SED 2016).

11 DATA AND RESOURCES

The results of this study can be found in The Site Characterization Database for Seismic Stations in Switzerland (SED 2016; <http://stations.seismo.ethz.ch>), where technical reports for each station can be directly retrieved. Related raw and processed data are available upon request to the SED.

ACKNOWLEDGEMENTS

The present work was made possible with the generous support of the NAGRA consortium and *Swissnuclear*. A special thank goes

also to Lorenz Keller (roXplore gmbh) and Giancarlo Dal Moro for their valuable contribution in performing the active seismic experiments. We also extend our thanks to Michael Asten, to the anonymous reviewer and to Editor Eiichi Fukuyama for all their insightful comments and valuable suggestions.

Map in Fig. 1 has been produced using Python basemap and the ESRI World Shaded Relief data available online on <http://server.arcgisonline.com>.

REFERENCES

- Anderson, J.G. & Hough, S.E. 1984. A model for the shape of the Fourier amplitude spectrum of acceleration at high-frequencies, *Bull. seism. Soc. Am.*, **74**, 1969–1993.
- Akkar, S., Sandikkaya, M.A. & Bommer, J.J., 2014. Empirical ground-motion models for point- and extended-source crustal earthquake scenarios in Europe and the Middle East, *Bull. Earthq. Eng.*, **12**, 359–387.
- Arai, H. & Tokimatsu, K., 2005. S-wave velocity profiling by joint inversion of microtremor dispersion curve and horizontal-to-vertical (H/V) spectrum, *Bull. seism. Soc. Am.*, **95**(5), 1766–1778.
- Arai, H. & Tokimatsu, K., 2004. S-wave velocity profiling by inversion of microtremor H/V spectrum, *Bull. seism. Soc. Am.*, **94**(1), 53–63.
- Asten, M.W., Askan, A., Ekincioglu, E.E., Sisman, F.N. & Ugurhan, B., 2014. Site characterisation in north-western Turkey based on SPAC and HVSR analysis of microtremor noise, *Explor. Geophys.*, **45**(2), 74–85.
- Asten, M.W. & Henstridge, J.D., 1984. Array estimators and the use of microseisms for reconnaissance of sedimentary basins, *Geophysics*, **49**(11), 1828–1837.
- Bergamo, P., Boiero, D. & Socco, L.V., 2012. Retrieving 2D structures from surface-wave data by means of space-varying spatial windowing, *Geophysics*, **77**(4), EN39–EN51.
- Boore, D.M. & Joyner, W.B., 1997. Site amplifications for generic rock sites, *Bull. seism. Soc. Am.*, **87**(2), 327–341.
- Bonnefoy-Claudet, S., Cotton, F. & Bard, P.-Y., 2006. The nature of noise wavefield and its applications for site effects studies: a literature review, *Earth-Sci. Rev.*, **79**(3–4), 205–227.
- Borcherdt, R.D., 1970. Effects of local geology on ground motion near San Francisco Bay, *Bull. seism. Soc. Am.*, **60**, 29–61.
- Burjánek, J., Edwards, B. & Fäh, D., 2014. Empirical evidence of local seismic effects at sites with pronounced topography: a systematic approach, *Geophys. J. Int.*, **197**, 608–619.
- Burjánek, J., Stamm, G., Poggi, V., Moore, J.R. & Fäh, D., 2010. Ambient vibration analysis of an unstable mountain slope, *Geophys. J. Int.*, **180**, 820–828.
- Capon, J., 1969. High resolution frequency wavenumber spectrum analysis, *Proc. IEEE*, **57**, 1408–1418.
- CEN., 2004. Eurocode 8: design of structures for earthquake resistance—Part 1: general rules, seismic actions and rules for buildings (EN 1998-1:), European Committee for Standardization.
- Claprod, M., Asten, M.W. & Kristek, J., 2011. Using the SPAC microtremor method to identify 2D effects and evaluate 1D shear-wave velocity profile in valleys, *Bull. seism. Soc. Am.*, **101**(2), 826–847.
- Claprod, M. & Asten, M.W., 2010. Statistical validity control on SPAC microtremor observations recorded with a restricted number of sensors, *Bull. seism. Soc. Am.*, **100**(2), 776–791.
- Cotton, F., Scherbaum, F., Bommer, J.J. & Bungum, H., 2006. Criteria for selecting and adjusting ground-motion models for specific target regions: applications to central Europe and rock sites, *J. Seismol.*, **10**(2), 137–156.
- Cranswick, E., 1988. The information content of high-frequency seismograms and the near-surface geologic structure of ‘hard rock’ recording sites, *Pageoph*, **128**, 333–363.
- Dal Moro, G., Keller, L. & Poggi, V., 2015. A comprehensive seismic characterisation via multi-component analysis of active and passive data, *First Break*, **33**(9), 45–53.
- Douglas, J. & Edwards, B., 2016. Recent and future developments in earthquake ground motion estimation, *Earth-Sci. Rev.*, **160**, 203–219.
- Douglas, J., 2003. Earthquake ground motion estimation using strong-motion records: a review of equations for the estimation of peak ground acceleration and response spectral ordinates, *Earth-Sci. Rev.*, **61**(1–2), 43–104.
- Edwards, B., Cauzzi, C., Danciu, L. & Faeh, D., 2016. Region-specific assessment, adjustment and weighting of ground motion prediction models: application to the 2015 Swiss Seismic Hazard Maps, *Bull. seism. Soc. Am.*, **106**(4), 1840–1857.
- Edwards, B., Ktenidou, O.-J., Cotton, F., Abrahamson, N., Van Houtte, C. & Fäh, D., 2015. Epistemic uncertainty and limitations of the k0 model for near-surface attenuation at hard rock sites, *Geophys. J. Int.*, **202**(3), 1627–1645.
- Edwards, B., Michel, C., Poggi, V. & Fäh, D., 2013. Determination of site amplification from regional seismicity: application to the Swiss National Seismic Networks, *Seismol. Res. Lett.*, **84**(4), 611–621.
- Edwards, B. & Fäh, D., 2013. A stochastic ground-motion model for Switzerland, *Bull. seism. Soc. Am.*, **103**, 78–98.
- Edwards, B., Poggi, V. & Fäh, D., 2011. A predictive equation for the vertical to horizontal ratio of ground-motion at rock sites based on shear wave velocity profiles: application to Japan and Switzerland, *Bull. seism. Soc. Am.*, **101**(6), 2998–3019.
- Ermert, L., Poggi, V., Burjanek, J. & Fäh, D., 2014. Fundamental and higher two-dimensional resonance modes of an Alpine valley, *Geophys. J. Int.*, **198**, 795–811.
- Fäh, D. et al., 2009. Determination of site information for seismic stations in Switzerland, Swiss Seismological Service Tech. Rept.: SED/PRP/R/004/20090831 for the Swiss-nuclear PEGASOS Refinement Project.
- Fäh, D., Stamm, G. & Havenith, H.-B., 2008. Analysis of three-component ambient vibration array measurements, *Geophys. J. Int.*, **172**, 199–213.
- Fäh, D., Kind, F. & Giardini, D., 2003. Inversion of local S-wave velocity structures from average H/V ratios, and their use for the estimation of site-effects, *J. Seismol.*, **7**, 449–467.
- Fäh, D., Kind, F. & Giardini, D., 2001. A theoretical investigation of average H/V ratios, *Geophys. J. Int.*, **145**(2), 535–549.
- Field, E.H., Johnson, P.A., Beresnev, I.A. & Zeng, Y., 1997. Nonlinear ground-motion amplification by sediments during the 1994 Northridge earthquake, *Nature*, **390**, 599–602.
- Garofalo, F. et al., 2016a. InterPACIFIC project: comparison of invasive and non-invasive methods for seismic site characterization. Part I: intra-comparison of surface wave methods, *Soil Dyn. Earthq. Eng.*, **82**, 222–240.
- Garofalo, F. et al., 2016b. InterPACIFIC project: comparison of invasive and non-invasive methods for seismic site characterization. Part II: inter-comparison between surface-wave and borehole methods, *Soil Dyn. Earthq. Eng.*, **82**, 241–254.
- Haghshenas, E., Bard, P.-Y., Theodulidis, N. & SESAME WP04 Team, 2008. Empirical evaluation of microtremor H/V spectral ratio, *Bull. Earthq. Eng.*, **6**(1), 75–108.
- Hayashi, K., Nozu, A. & Tanaka, M., 2011. Joint inversion of three-component microtremor measurements and microtremor array measurements at Mexico City, *SEG Technical Program Expanded Abstracts*, pp. 917–921, doi:10.1190/1.3628222.
- Hobiger, M., Fäh, D., Scherrer, C., Michel, C., Duvernay, B., Clinton, J., Cauzzi, C. & Weber, F., 2017. The renewal project of the swiss strong motion network (SSMNet), in *Proceedings of the 16th World Conference on Earthquake Engineering (16WCEE)*, Santiago de Chile, 2017 January 9 to 13.
- Hollender, F. et al., 2017. Characterization of site conditions (soil class, VS30, velocity profiles) for 33 stations from the French permanent accelerometric network (RAP) using surface-wave methods, *Bull. Earthq. Eng.* doi:10.1007/s10518-017-0135-5.
- Horiike, M., 1985. Inversion of phase velocity of long-period microtremors to the S-wave-velocity structure down to the basement in urbanized areas, *J. Phys. Earth*, **33**, 59–96.
- Ikeda, T., Asten, M.W. & Matsuoka, T., 2013. Joint inversion of spatial autocorrelation curves with HVSR for site characterization in Newcastle,

- Australia, in *Proceedings of the 23rd ASEG International Geophysical Conference and Exhibition*, Melbourne, Australia.
- Joyner, W.B., Warrick, R.E. & Fumal, T.E., 1981. The effect of quaternary alluvium on strong ground motion in the coyote lake, california, earthquake of 1979, *Bull. seism. Soc. Am.*, **71**, 1333–1349.
- Knopoff, L., 1964. A matrix method for elastic wave problems, *Bull. seism. Soc. Am.*, **54**, 431–438.
- Manea, E.F., Michel, C., Poggi, V., Fäh, D., Radulian, M. & Balan, F., 2016. Improving the shear wave velocity structure beneath Bucharest (Romania) using ambient vibrations, *Geophys. J. Int.*, **207**(2), 848–861.
- Maranò, S., Fäh, D. & Lu, Y.M., 2014. Sensor placement for the analysis of seismic surface waves: sources of error, design criterion and array design algorithms, *Geophys. J. Int.*, **197**(3), 1566–1581.
- Matsushima, S., Hirokawa, T., De Martin, F., Kawase, H. & Sanchez-Sesma, F.J., 2014. The effect of lateral heterogeneity on horizontal-to-vertical spectral ratio of microtremors inferred from observation and synthetics, *Bull. seism. Soc. Am.*, **104**(1), 381–393.
- Michel, C., Fäh, D., Edwards, B. & Cauzzi, C., 2017. Site amplification at the city scale in Basel (Switzerland) from geophysical site characterization and spectral modelling of recorded earthquakes, *Phys. Chem. Earth*, **98**, 27–40.
- Michel, C., Edwards, B., Poggi, V., Burjánec, J., Roten, D., Cauzzi, C. & Fäh, D., 2014. Assessment of site effects in alpine regions through systematic site characterization of seismic stations, *Bull. seism. Soc. Am.*, **104**(6), 2809–2826.
- Nakamura, Y., 1989. A method for dynamic characteristics estimation of subsurface using microtremor on the ground surface, *Quart. Records Railway Tech. Res. Inst.*, **30**, 25–33.
- Nogoshi, M. & Igarashi, T., 1971. On the amplitude characteristics of microtremor, Part II, *J. seism. Soc. Japan*, **24**, 26–40.
- Okada, H., 2003. *The Microtremor Survey Method*, eds. Fitterman, D.V. & Asten, M.W., Society of Exploration Geophysicists.
- Parolai, S., Picozzi, M., Richwalski, S.M. & Milkereit, C., 2005. Joint inversion of phase velocity dispersion and H/V ratio curves from seismic noise recordings using a genetic algorithm, considering higher modes, *Geophys. Res. Lett.*, **32**(1), 1–4.
- Pileggi, D., Rossi, D., Lunedei, E. & Albarello, D., 2011. Seismic characterization of rigid sites in the ITACA database by ambient vibration monitoring and geological surveys, *Bull. Earthq. Eng.*, **9**(6), 1839–1854.
- Picozzi, M. & Albarello, D., 2007. Combining genetic and linearized algorithms for a two-step joint inversion of Rayleigh wave dispersion and H/V spectral ratio curves, *Geophys. J. Int.*, **169**(1), 189–200.
- Poggi, V., Edwards, B. & Fäh, D., 2013. Reference S-wave velocity profile and attenuation models for ground-motion prediction equations: application to Japan, *Bull. seism. Soc. Am.*, **103**(5), 2645–2656.
- Poggi, V., Edwards, B. & Fäh, D., 2012a. Characterizing the vertical to horizontal ratio of ground-motion at soft sediment sites, *Bull. seism. Soc. Am.*, **102**(6), 2741–2756.
- Poggi, V., Fäh, D. & Giardini, D., 2012b. T-*f-k* analysis of surface waves using the continuous wavelet transform, *Pure appl. Geophys.*, **170**(3), 319–335.
- Poggi, V., Fäh, D., Burjánec, J. & Giardini, D., 2012c. The use of Rayleigh wave ellipticity for site-specific hazard assessment and microzonation. An application to the city of Luzern (Switzerland), *Geophys. J. Int.*, **188**(3), 1154–1172.
- Poggi, V., Edwards, B. & Fäh, D., 2011. Derivation of a reference shear-wave velocity model from empirical site amplification, *Bull. seism. Soc. Am.*, **101**, 258–274.
- Poggi, V. & Fäh, D., 2010. Estimating rayleigh wave particle motion from three-component array analysis of ambient vibrations, *Geophys. J. Int.*, **180**(1), 251–267.
- Renalier, F., Jongmans, D., Savvaidis, A., Wathelet, M., Endrun, B. & Cornou, C., 2010. Influence of parameterization on inversion of surface wave dispersion curves and definition of an inversion strategy for sites with a strong contrast, *Geophysics*, **75**, B197–B209.
- Richart, F.E., Hall, J.R. & Woods, R.D., 1970. *Vibrations of Soils and Foundations*, Prentice-Hall, Inc.
- Roberts, J. & Asten, M.W., 2008. A study of near source effects in array-based (SPAC) microtremor surveys, *Geophys. J. Int.*, **174**, 159–177.
- Roten, D. & Fäh, D., 2007. A combined inversion of Rayleigh wave dispersion and 2-D resonance frequencies, *Geophys. J. Int.*, **168**, 1261–1275.
- Sambridge, M., 1999. Geophysical inversion with a neighbourhood algorithm: I. Searching a parameter space, *Geophys. J. Int.*, **138**, 479–494.
- SED - Swiss Seismological Service, ETH Zurich, 2016. The Site Characterization Database for Seismic Stations in Switzerland, Federal Institute of Technology, Zurich. <http://dx.doi.org/10.12686/sed-stationcharacterizationdb> retrieved on 04/02/2016 from <http://stations.seismo.ethz.ch>.
- SED - Swiss Seismological Service, ETH Zurich, 2015. Swiss National Probabilistic Seismic Hazard Assessment 2015, Federal Institute of Technology, Zurich, retrieved on 31/01/2017 from <http://www.seismo.ethz.ch/en/knowledge/seismic-hazard-switzerland/>.
- Tucker, B.E., King, J.L. & Neresov, I.L., 1984. Observations of hard-rock site-effects, *Bull. seism. Soc. Am.*, **74**, 137–151.
- Wathelet, M., Jongmans, D., Ohrnberger, M. & Bonnefoy-Claudet, S., 2008. Array performances for ambient vibrations on a shallow structure and consequences over Vs inversion, *J. Seismol.*, **12**(1), 1–19.
- Wathelet, M., 2008. An improved neighborhood algorithm: parameter conditions and dynamic scaling, *Geophys. Res. Lett.*, **35**(9), 1–5.
- Wiemer, S. *et al.*, 2016. Seismic Hazard Model 2015 for Switzerland (SUH2015), Official Report of the Swiss Seismological Service, doi: 10.12686/a2.
- Xia, J., Miller, R.D. & Park, C.B., 1999. Estimation of near-surface shear-wave velocity by inversion of Rayleigh wave, *Geophysics*, **64**, 691–700.

SUPPORTING INFORMATION

Supplementary data are available at *GJI* online.

Figure S1. Surface-to-borehole spectral ratios (SSR) compared to ratios of empirical spectral modelling (ESM) amplification functions and SH-waves transfer function (SHTF) from the retrieved 1-D velocity profiles, including the mean plus/minus one standard deviation for stations STIEG, HAMIK and BOBI.

Please note: Oxford University Press is not responsible for the content or functionality of any supporting materials supplied by the authors. Any queries (other than missing material) should be directed to the corresponding author for the paper.